

Analysis and design of microwave resonant plasma source for Iranian Space Plasma Simulation Chamber

Hamid Reza Mirzaei^{1*}, Moslem Kazemi², Gholamreza Etaati², Milad Abbasi³, Mahmood Karimi Kafshgari⁴, Hosein Rajabalinia Jelodar⁴

Abstract

In the present study, the microwave resonant plasma source has been designed to provide the ionosphere like condition inside the Iranian Space Plasma Simulation Chamber (ISPSC). This chamber contains plasma with electron density of $1 \times 10^5 - 1 \times 10^{10} \text{ cm}^{-3}$ and temperature of 1-5 eV. In order to reach these plasma parameters inside the ISPSC, the plasma source cylindrical cavity mode TE_{112} is used. Then, the produced plasma is transferred into the Chamber through the holes created on the end wall of the cavity. Since the plasma characteristics in the resonant cavity depend on the gas pressure and the input power, the microwave and plasma interaction, power absorption, electron density and temperature were evaluated by the Comsol Multiphysics and obtained results have been presented.

Keywords

Plasma source, Cavity, Comsol, Space plasma.

¹ Department of Physics and Accelerators, Nuclear Science and Technology Research Institute (NSTRI), Tehran, Iran

² Physics and Energy Engineering Department, Amirkabir University, Tehran, Iran

³ Plasma Research Institute, University of Shahid Beheshti, Tehran, Iran

⁴ Plasma Physics Research Center, Science and Research Branch, Islamic Azad University, Tehran, Iran

*Corresponding author: hamidreza.mirzaei@aut.ac.ir

1. Introduction

The space plasma simulation devices were constructed to provide similar plasmas like space plasma and they have the main role of investigate the fundamental physics of space plasmas like space plasma waves and instability, modeling the earth's and planetary space environments, simulation of the ionospheric heating, magnetic field generation and reconnection [1, 2].

Many space plasma devices were designed and constructed such as Large Plasma Device (LAPD) [2], Navy Research Laboratory Space Physics Simulation Chamber (NRL-SPSC) [3], Magnetic Reconnection Experiment (MRX) [4], KROX device [5], Space Environment Simulation Research Infrastructure (SESRI) [6], Facility for Laboratory Reconnection Experiment (FLARE) [7], Keda Space Plasma Experiment (KSPEX) [8], Madison Plasma Dynamo eXperiment (MPDX) [9] and Versatile Instrument for studies on Nonlinearity, Electromagnetism, Turbulence, and Application II (VINETA II) [10].

For space plasma investigation and devices many sources were used like DC discharge (thermionic emission [3, 11, 12] or heated oxide-coated cathodes [13, 14]), Radio Frequency (RF) discharges [15–17], microwave discharge [9, 18, 19]. Nowadays plasma sources based on microwave were developed because of the simplicity, choice of the different gases, and ease of operation. There were many types of plasma sources based on microwave.

The Iranian Space Plasma Simulation Chamber, a large, linear plasma research device that has been designed and is under construction to study space plasma physics. In this paper design and construction of the large volume microwave plasma source based on the resonant cavity were described. This plasma source device is designed to provide a plasma with characteristic close to space plasma.

This paper is organized as follows. Section 2 deals with the introduce of ISPSC and plasma source. Design and simulation considerations of microwave plasma source are presented in Section 3. The obtained results are reported and discussed in Section 4. Finally, Section 5 provides a summary and conclusions.

2. Iranian Space Plasma Simulation Chamber

A space plasma simulation chambers are a large vacuum device appropriate to produce and retain the plasma. This plasma is produced by plasma sources connected to the chamber that is capable to provide a plasma with space plasma like characteristics.

A space plasma simulation chambers are used to perform studies and simulations for plasma physic, ionosphere and magnetosphere. Also, the chamber is appropriate to test the satellite, thruster, electronic board, space-borne instruments and sensors used in the ionosphere. Another usage of this

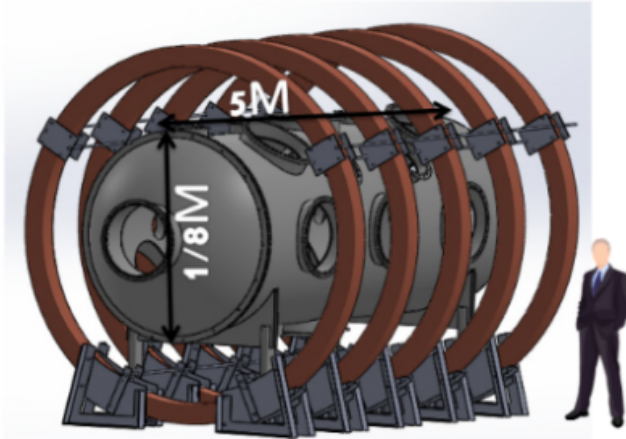


Figure 1. The Iranian Space Plasma Simulation Chamber.

facility is for calibration and test of the plasma diagnostics because therefore, the chamber should be large enough that the tested and diagnostic devices not be influenced by the plasma source or the chamber walls.

Iranian Space Plasma Simulation Chamber (ISPSC) is under construction and will be operational soon. The schematic ISPSC was shown in Figure 1. This is a large device that produces the environment with quiescent plasma and consists of a large volume chamber (a cylinder of length 5 m and diameter of 1.8 m) equipped with a plasma source, vacuum system, magnetic coils and several diagnostic tools.

The chamber has 32 ports to ensure excellent access for diagnostics and other systems. The vacuum system includes Rotary pump, Roots Pump, Turbomolecular pump and Cryogenic Pump. The ultimate pressure and working pressure are 10^{-6} and 10^{-4} Torr, respectively. This machine is surrounded by a set of 5 magnetic coils which can generate an axial magnetic field up to 150 G. The plasma is monitored by Langmuir Probe, Optic Emission Spectrometry, Interferometry and so on. In addition, the cylindrical resonant cavity design and characterization as a microwave plasma source for this device has been reported in the present study.

3. Design and simulation considerations of plasma source

In order to equip the ISPSC with the plasma source, the magnetron based microwave cavity source has been selected. The Radio Frequency (RF) plasma sources were attractive because unlike the filament source, they have equal ion and electron production rate. Also the RF inductive and capacitive discharge weren't suitable and these sources should be introduced to the experimental region. Also Electron Cyclotron Resonance (ECR) plasma source wasn't chosen because it produces plasma denser than required.

As considerations, the source should have a large size and constant ionization rate. As the ISPSC size, the source diameter would be near 40 cm. The depth of the cylindrical

cavity is determined by the resonant mode and magnetron frequency. Whereas the magnetron frequency is fixed (2.45GHz), a resonance mode that generates a constant electric field as a function of the radius was selected. We choose a TE_{112} cylindrical cavity mode. The frequency of a TE mode resonance in cylindrical cavity is given by [20]

$$f_{TE_{nm}} = \frac{c}{2\pi} \left(\frac{q'_{nm}}{R^2} + \frac{l^2 \pi^2}{L^2} \right)^{1/2} \quad (1)$$

where c is the speed of light and q'_{nm} is the zero of the derivative of the Bessel function. We settled on a TE_{112} cylindrical cavity mode whose electric field components for $n=1, m=1, l=2, R=35.6$ cm and $q_{11}=1.841$ is the first zero of the Bessel function.

The cavity was designed to have a somewhat lower resonant frequency than the magnetron frequency in order that cavity tuning could occur. An increase in the resonant frequency occurs when volume in the cavity is displaced by the stub. In this source, the cavity length (L) is 12.35 cm and the resonant frequency of the TE_{112} mode becomes 2.41 GHz. By increase of 0.15 cm to the overall cavity length, the center frequency reach 2.45 GHz. The center frequency of cavity is 40 MHz below the expected center frequency of the magnetron (2.45 ± 0.01 GHz) and allows for cavity tuning by stub adjustment. The stub tuning is a cylindrical (diameter ~ 10.2 cm, $L \sim 2.5$ cm) that is attached to NW 16 ports.

Figure 2 shows the schematics of the cavity and other parts with dimensions. The cavity was constructed from a single piece of aluminum. The backplate was attached to the open face of cavity and mounted between the cavity and chamber. The holes (21 holes, $D=0.38$ cm) were drilled into the plate to provide the plasma access to the chamber. The plasma was diffused from the cavity to the chamber through these holes because of the differential pressure and magnetic field.

In the present work, COMSOL Multi-physics software has been used for the simulation. This software has the capability to simulate a Microwave discharge plasma. The microwave-plasma module was used for electron density and energy calculations. The microwave-plasma module for electron density and energy calculations method have been employed.

$$\nabla \times \mu^{-1} (\nabla \times E) - k_0^2 (\epsilon_r - \frac{i\sigma}{\omega \epsilon_0}) E = 0 \quad (2)$$

where, σ is the plasma conductivity tensor, E is the electric field, k_0 is the wave number of free space, ϵ_r is the relative dielectric tensor, ω is the angular wave frequency, and ϵ_0 is the permittivity of vacuum. In this model, microwave equations are solved in the frequency domain and all other parameters in the time domain. The electron density (or plasma density) and mean electron energy are computed by solving a pair of drift-diffusion equations for the electron density and mean electron energy.

$$\frac{\partial}{\partial t} (n_e) + \nabla \cdot [-n_e (\mu_e \cdot E) - D_e \cdot \nabla n_e] = R_e \quad (3)$$

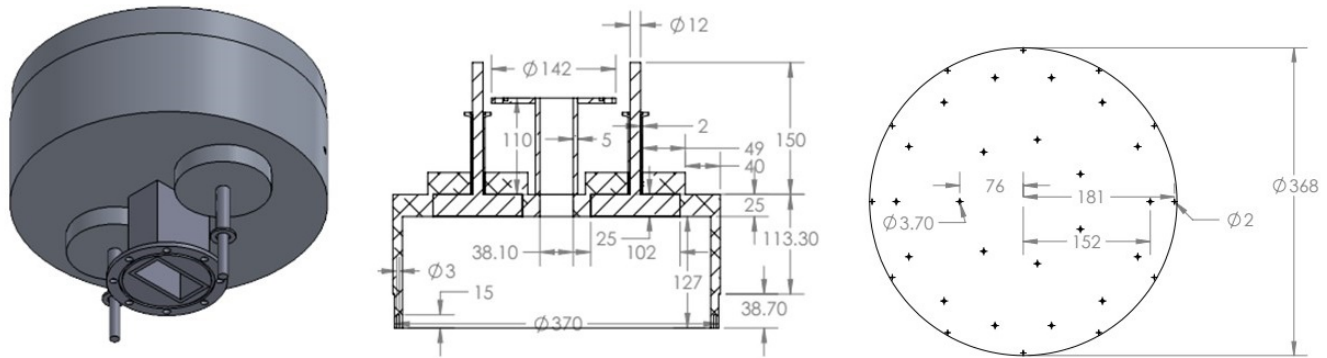


Figure 2. The schematics of the microwave resonant plasma source (diameter~35.6 cm, $L \sim 12.35$ cm), tuning stubs and backplate with dimensions.

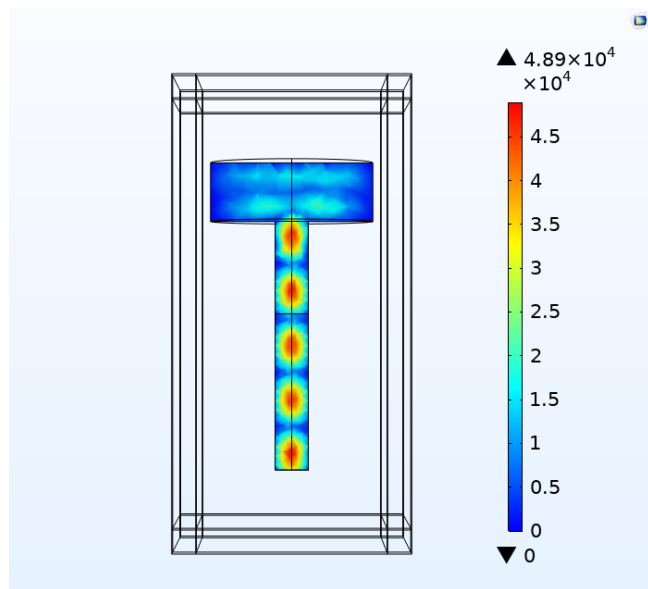


Figure 3. The magnitude of the electric field produced by the TE_{112} mode for 2.41 GHz and 800 W input power.

$$\frac{\partial}{\partial t}(n_e) + \nabla \cdot [-n_e(\mu_e \cdot E) - D_e \cdot \nabla n_e] + E \cdot \Gamma_e = R_e \quad (4)$$

where $E \cdot \Gamma_e = en_e v_e \cdot E_{ambipolar} - \Pi$. The heating term $E \cdot \Gamma_e$ has two components. The first part gives energy to electrons by means of the ambipolar field. The second part (Π) is the absorbed power ($n_e < v_e \cdot \vec{E}$) the electrons due to microwave. Here, n_e , v_e , R_e , Γ_e , μ_e , E , D_e , n_e , R_e , Γ_e and D_e are the electron density, mean electron velocity, electron source term, electron flux, electron mobility, electron energy mobility, total electric field, electron diffusivity, electron energy density, energy loss/gain due to inelastic collisions, electron energy flux, electron energy mobility and electron energy diffusivity, respectively. The plasma chamber wall is grounded. The reflections as well as secondary emission and thermal emission of the electrons are neglected at the wall boundaries.

The equation-based mesh user-controlled mesh is employed

to create an extremely fine mesh size on the plasma chamber and a fine mesh size on the waveguide. The maximum and minimum mesh element size on different edges of computational domain are 0.5 mm and 0.0055 mm, respectively. The number of degrees of freedom solved for time dependent solver of the Microwave plasma model is 37598.

4. Results and discussion

Three-dimensional simulations were performed to analyze the microwave discharge by modeling the microwaves-plasma interaction. With this aim, the computational domain consisted of a cylindrical cavity (diameter~35.6 cm, $L \sim 12.35$ cm), as well as a microwave injection WR284 waveguide operating in TE_{10} mode of 2.45 GHz. The cavity walls had been assumed as the perfect electric conduction.

The magnitude of the electric field in the cavity for 2.41 GHz and 800 W input power has been calculated as shown in Figure 3. This shows the TE_{112} mode has been excited on the cavity.

In the following, the impact of the filling gas pressure on the electric field strength, power absorption and reflection as well as plasma density have been investigated theoretically. Argon was chosen as the filling gas. This gas can absorb some portions of the microwave power while reflecting the rest of it due to plasma generation leading to a total power reduction in the waveguide. Because of this power absorption and reflection, an amount of electric field energy would be stored in the chamber. The microwave propagation and absorption have been simulated.

The distribution of the absorbed microwave power for 0.01 and 0.05 ms was shown in Figure 4. These show that the microwave power was absorbed in a high electric field of the cavity and then absorption region was changed because of the dense plasma was formed. It is clear from the figure that the sharp gradient of the electric field indicates power absorption that leads to plasma generation.

In addition, with a comparison of the electric field along the waveguide before plasma formation as presented in Figure 3, and in the presence of plasma illustrated in Figure 5, it can

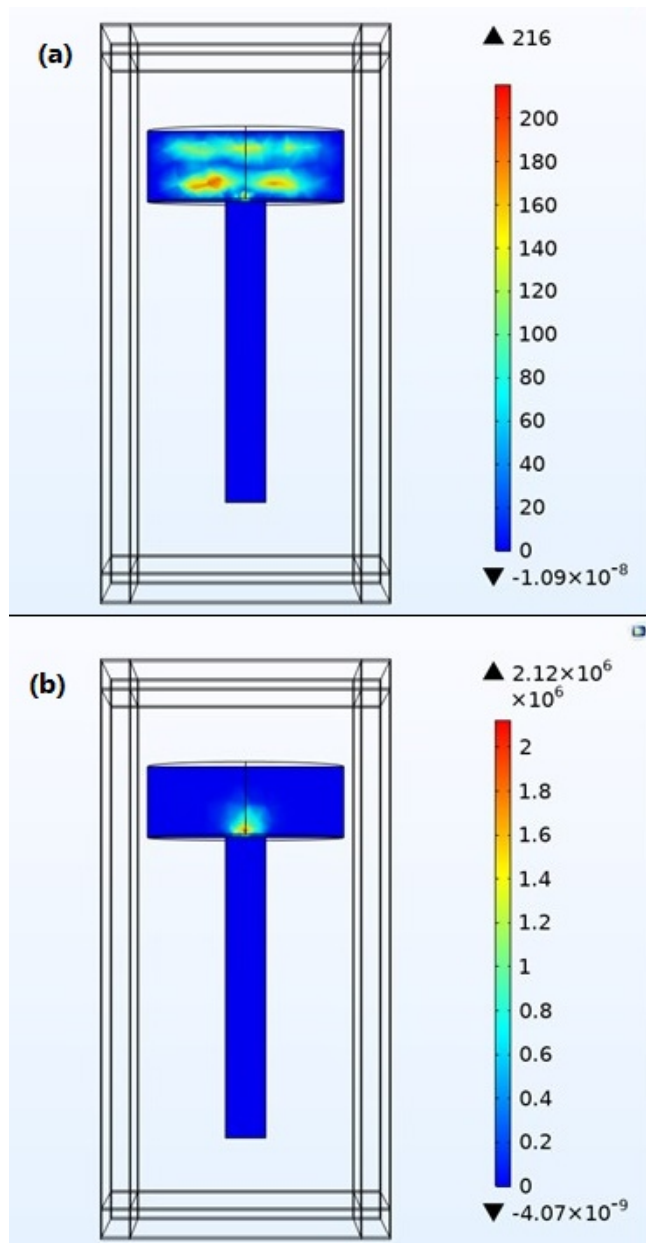


Figure 4. Distribution of absorbed microwave power (W/m^3) into the plasma at 0.05 Pa and with 800 W input microwave power for a) $t = 0.01$ and 0.05 ms.

be found that the electric field in the waveguide has also been reduced. At this time S_{11} was -2 dB. This impact is severe due to the generation of a local dense plasma with the high reflection of the power.

It is worth mentioning that, the reflection power along the waveguide, as well as cavity, should be adjusted by the stub tuner.

It can be seen from Figure 6 that the peak electron density at 0.05 Pa is around $7 \times 10^{16} m^{-3}$ that is below the critical plasma density ($7.4 \times 10^{16} m^{-3}$ at 2.45 GHz). In addition, the electron temperature and plasma potential have been

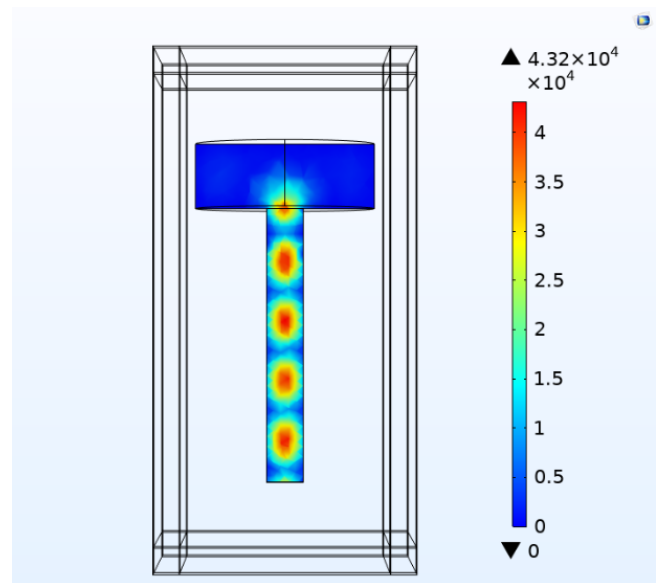


Figure 5. Distribution of the microwave electric field in the presence of plasma at 0.05 Pa and with 800 W input microwave for $t = 0.05$ ms.

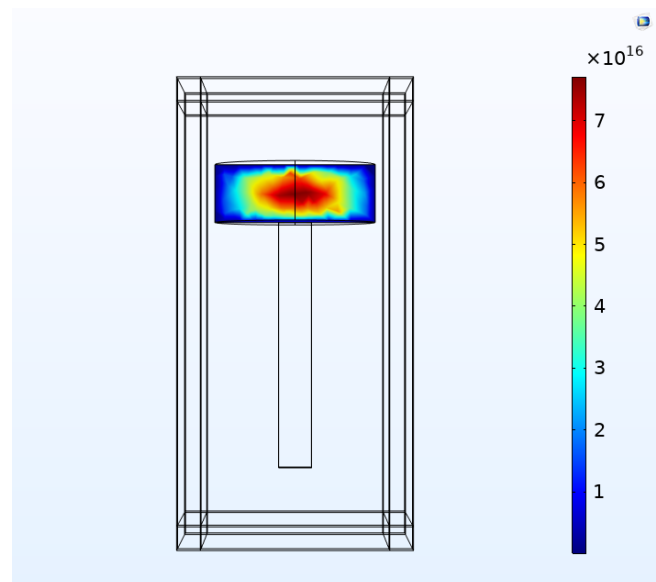


Figure 6. The electron density of plasma at 0.05 Pa and with 800 W input microwave.

also calculated. The obtained results are illustrated in Figure 7 and 8. Figures show that the electron temperature were 12 eV and the plasma potential has peaks around 40 V that is about 7 times the maximum electron temperature. The plasma potential is uniform throughout the plasma, even though the electron temperature shows large variations. It is confirmed by the expression of the classical sheath theory that is $\phi/T_e = \ln(m_i/2\pi m_e)/2 + 1 = 5.7$ for low-pressure Argon plasmas.

For further analysis, electron density and temperature for different pressures are given in Figure 9 and 10, respectively. An

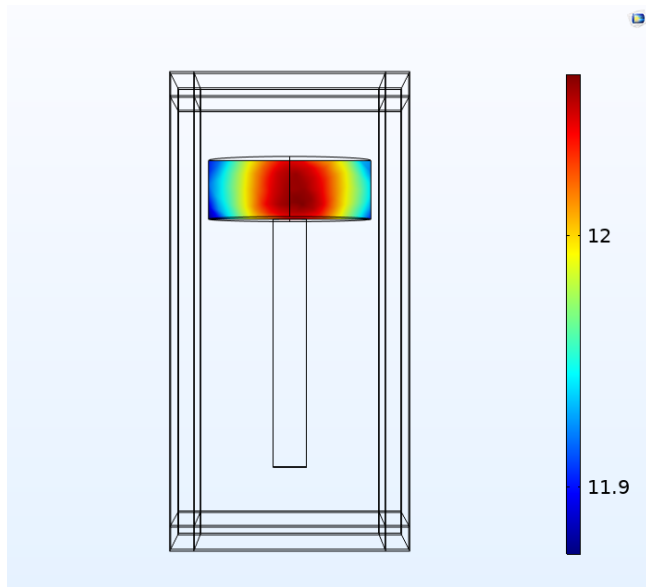


Figure 7. The electron temperature of plasma at 0.05 Pa and with 800 W input microwave.

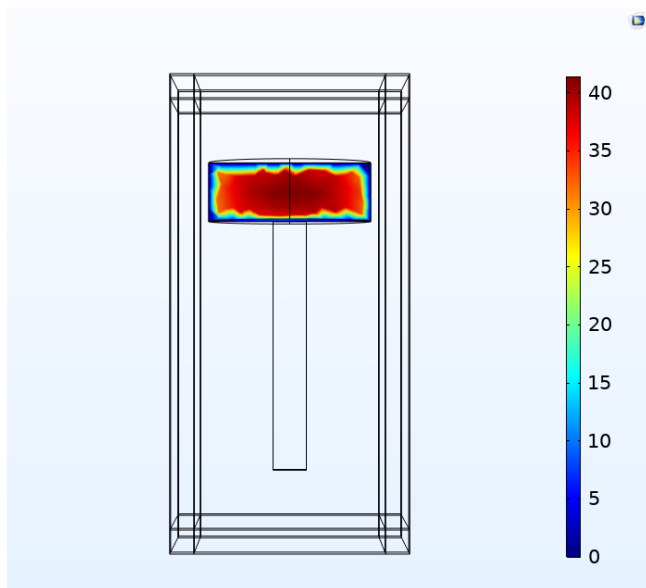


Figure 8. The electric potential of plasma at 0.05 Pa and with 800 W input microwave.

increase in density and a drop in temperature to a pressure of 06 Pascals is evident.

The obtained results from the calculations show that the plasma with a density of $7 \times 10^{16} \text{ m}^{-3}$ and a temperature of 12 eV via the designed resonant cavity plasma source can be provided. Then, the produced plasma is transferred into the chamber through the holes created on the end wall of the cavity. Therefore, the plasma with an electron density of $1 \times 10^5 - 1 \times 10^{10} \text{ cm}^{-3}$ and temperature of 1-5eV inside the ISPSC is achievable. Also, the study showed that this plasma source has an appropriate performance at different working

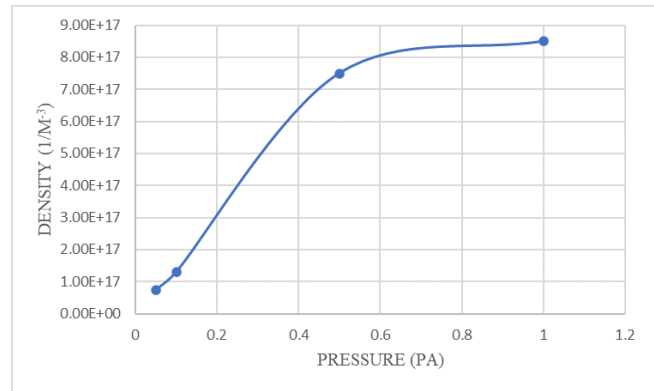


Figure 9. The electron density of plasma with 800 W input microwave for different pressures.

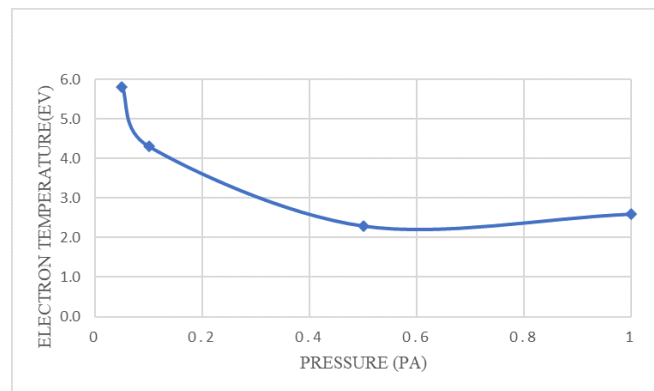


Figure 10. The electron temperature of plasma with 800 W input microwave for different pressures.

pressures. As a result, the designed device has the necessary capabilities to be used in the ISPSC.

5. Conclusion

In the present paper, the resonant cavity plasma source had been designed to produce space plasma like inside ISPSC. This is a cylindrical cavity with a diameter of 35.6 and length of 12.35 cm, as well as a microwave injection WR284 waveguide operating in TE10 mode of 2.45 GHz.

Since the plasma characteristics in the resonant cavity depend on the gas pressure and the input power, the microwave and plasma interaction, power absorption, electron density, and temperature were evaluated by the Comsol Multiphysics and obtained results have been presented.

The obtained results showed that the designed resonant cavity plasma source produces plasma with $7 \times 10^{16} \text{ m}^{-3}$ and 12 eV electron density and temperature, respectively. Therefore, the plasma with an electron density of $1 \times 10^5 - 1 \times 10^{10} \text{ cm}^{-3}$ and temperature of 1-5eV inside the ISPSC is achievable.

Due to the large dimensions of the plasma source and its performance in different working pressures and production of desired plasma density and temperature, the designed resonant cavity plasma source is appropriate for use in the ISPSC.

Conflict of interest statement:

The authors declare that they have no conflict of interest.

References

- [1] Y. Liu, P. Shi, X. Zhang, J. Lei, and W. Ding. *Review of Scientific Instruments*, **92**:071101, 2021.
- [2] W. Gekelman, H. Pfister, Z. Lucky, J. Bamber, D. Leneman, and J. Maggs. *Review of scientific instruments*, **62**:2875, 1991.
- [3] W. Amatucci, G. Ganguli, D. Walker, G. Gatling, M. Balkey, and T. McCulloch. *Physics of Plasmas*, **10**:1963, 2003.
- [4] M. Yamada and H. Ji. *American Astronomical Society Meeting Abstracts*, **194**:31, 1999.
- [5] N. A. Aidakina, A. G. Galka, V. I. Gundorin, M. E. Gushchin, I. Yu. Zudin, S. V. Korobkov, A. V. Kostrov, K. N. Loskutov, M. M. Mogilevskiy, S. E. Priver, A. V. Strikovskiy, D. V. Chugunin, and D. V. Yanin. *Geomagnetism and Aeronomy*, **58**:314, 2018.
- [6] X. Qingmei, W. Zhibin, E. Peng, W. Xiaogang, X. Chijie, R. Yang, J. I. Hantao, M. Aohua, and L. I. Liyi. *Plasma Science and Technology*, **19**:055302, 2017.
- [7] P. A. Melnik, A. H. Bushnell, P. E. Sieck, J. E. Stuber, S. Woodruff, F. Hoffmann, J. JaraAlmonte, H. Ji, M. Kalish, A. Zhao, T. E. Ziemba, and K. E. Miller. *International Power Modulator and High Voltage Conference*, :635, 2016.
- [8] Y. Liu, Z. Zhang, J. Lei, J. Cao, P. Yu, X. Zhang, L. Xu, and Y. Zhao. *Review of Scientific Instruments*, **87**:093504, 2016.
- [9] C. M. Cooper, J. Wallace, M. Brookhart, M. Clark, C. Collins, W. X. Ding, K. Flanagan, I. Khalzov, Y. Li, J. Milhone, M. Nornberg, P. Nonn, D. Weisberg, D. G. Whyte, E. Zweibel, and C. B. Forest. *Physics of Plasmas*, **21**:013505, 2014.
- [10] H. Bohlin, A. Von Stechow, K. Rahbarnia, O. Grulke, and T. Klinger. *Review of Scientific Instruments*, **85**:023501, 2014.
- [11] A. DuBois, I. Arnold, E. Thomas Jr, E. Tejero, and W. Amatucci. *Review of Scientific Instruments*, **84**:43503, 2013.
- [12] Z. Ulibarri, J. Han, M. Horányi, T. Munsat, X. Wang, G. Whittall-Scherfee, and L. H. Yeo. *Review of Scientific Instruments*, **88**:115112, 2017.
- [13] G. Hu, X. Jin, L. Yuan, Q. Zhang, J. Xie, H. Li, and W. Liu. *Plasma Science and Technology*, **18**:918, 2016.
- [14] D. Leneman, W. Gekelman, and J. Maggs. *Review of scientific instruments*, **77**:015108, 2006.
- [15] X. Zhang, J.-X. Cao, Y. Liu, Y.-P. Wang, P.-C. Yu, and Z.-K. Zhang. *IEEE Transactions on Plasma Science*, **45**:338, 2017.
- [16] E. E. Scime, P. A. Keiter, M. M. Balkey, J. L. Kline, X. Sun, A. M. Keesee, R. A. Hardin, I. A. Biloiu, S. Houshmandyar, S. Chakraborty Thakur, J. Carr Jr., M. Galante, D. McCarren, and S. Sears. *Journal of Plasma Physics*, **81**, 2015.
- [17] M. E. Gushchin, T. M. Zaboronkova, V. A. Koldanov, S. V. Korobkov, A. V. Kostrov, C. Krafft, , and A. V. Strikovskiy. *Physics of Plasmas*, **15**:023504, 2008.
- [18] J. H. Bowles, D. Duncan, D. N. Walker, W. E. Amatucci, and J. A. Antoniadis. *Review of scientific instruments*, **67**:455, 1996.
- [19] Z. Zhang, Y. Liu, J. Cao, P. Yu, X. Zhang, and J. Wang. *Review of Scientific Instruments*, **90**:103502, 2019.
- [20] D. M. Pozar. *Microwave engineering*. John Wiley and sons, 4th edition, 2011.